Journal of Cranio-Maxillo-Facial Surgery 47 (2019) 1739–1751

Contents lists available at ScienceDirect

Journal of Cranio-Maxillo-Facial Surgery

journal homepage: www.jcmfs.com

Differential regulation of blood vessel formation between traumatic temporomandibular joint fibrous ankylosis and bony ankylosis in a sheep model

Su-Xia Liang [a, 1], Hua-Lun Wang [b, 1], Pei-Pei Zhang [b], Jun Shen [b], Kun Yang [b], Li Meng [b], Hao Liu [b], Ying-Bin Yan [b, *]

[a] Department of Operative Dentistry and Endodontics, Tianjin Stomatological Hospital, 75 Dagu Road, Heping District, Tianjin 300041, PR China
[b] Department of Oromaxillofacial-Head and Neck Surgery, Tianjin Stomatological Hospital, 75 Dagu Road, Heping District, Tianjin 300041, PR China

ARTICLE INFO

Article history:
Paper received 17 March 2019
Accepted 28 July 2019
Available online 1 August 2019

Keywords:
Temporomandibular joint
Fibrous ankylosis
Bony ankylosis
Trauma
Animal model
Angiogenesis

ABSTRACT

Objectives: Clinical and experimental studies show that the etiology of traumatic temporomandibular joint (TMJ) fibrous ankylosis and bony ankylosis are associated with the severity of trauma. However, how the injury severity affects the tissue differentiation is not clear. We tested the hypothesis that angiogenesis affects the outcomes of TMJ trauma, and that enhanced neovascularization after severe TMJ trauma would promote the development of bony ankylosis.

Methods: Bilateral condylar sagittal fracture and discectomy were performed for each sheep, with the glenoid fossa receiving either severe trauma to induce bony ankylosis or minor trauma to induce fibrous ankylosis. At days 7, 14, 28, and 56 after surgery, total RNA was extracted from the ankylosed callus. Temporal gene expressions of several molecules functionally important for blood vessel formation were studied by real-time PCR.

Results: Histological examination revealed a prolonged hematoma phase and a lack of cartilage formation in fibrous ankylosis. mRNA expression levels of HIF-1α, VEGF, VEGFR2, SDF1, Ang1, Tie2, vWF, CYR61, FGF2, TIMP1, MMP2, and MMP9 were distinctly lower in fibrous ankylosis compared with bony ankylosis at several time points.

Conclusions: Our study indicates that inhibition of angiogenesis after TMJ trauma might be a promising strategy for preventing bony ankylosis in the future.

1. Introduction

Traumatic temporomandibular joint (TMJ) ankylosis, manifesting as progressively restricted mouth opening and masticatory difficulty, is a severe complication secondary to TMJ trauma, although the incidence of it is only 0.4–2% (Laskin, 1978). Treatment of the condition poses a significant challenge because of the difficulties of operative management and the high incidence of recurrence (Valentini et al., 2002).

The pathological process and pathogenesis of traumatic TMJ ankylosis have generated great interest among craniomaxillofacial surgeons, yet remain an enigma. A better understanding of its molecular pathophysiology may offer better approaches for its prevention, diagnosis, and treatment at the molecular level (Yan et al., 2014b). The difficulty in acquiring clinical specimens of TMJ ankylosis impedes research in this field, although several authors have attempted to explore the cellular mechanisms using human samples (Xiao et al., 2013; He et al., 2015). In addition, specimens from patients can only represent the end stage of the disease, rather than the onset, the early stages, or the whole development process of the condition. Therefore, animal models are essential components of research into TMJ ankylosis.

To date, an animal model that is widely accepted and mimics human disease exactly has not been established. In our previous study, a reliable sheep model of TMJ ankylosis through condylar

* Corresponding author.
E-mail addresses: lliangyuer@163.com (S.-X. Liang), 870160795@qq.com (H.-L. Wang), 1124889616@qq.com (P.-P. Zhang), 13902143866@163.com (J. Shen), 625044317@qq.com (K. Yang), 843153290@qq.com (L. Meng), kqlh2013@163.com (H. Liu), yingbinyan@qq.com (Y.-B. Yan).
[1] The first two authors contributed equally to this paper.

https://doi.org/10.1016/j.jcms.2019.07.032
1010-5182/

sagittal fracture, damage to the glenoid fossa, and removal of the lateral 2/3 disc was developed (Yan et al., 2013), and provided a useful medium for studying the molecular pathogenesis of the disease (Yan et al., 2014b and 2014a). An interesting finding from the sheep model was that minor trauma to the glenoid fossa led to fibrous ankylosis both at 3 months and 6 months after surgery, whereas severe trauma to the glenoid fossa resulted in fibro-osseous ankylosis at 1 month and 3 months postoperatively, and ultimately bony ankylosis at 6 months postoperatively (Yan et al., 2013). These findings suggested a couple of things. Firstly, bony ankylosis and fibrous ankylosis might be the result of two different pathological processes, and bony ankylosis might only evolve from fibro-osseous ankylosis. This differed from the traditional view that both fibrous and bony ankylosis were variations of the same pathology (Miller et al., 1975). Secondly in the sheep model the degree of injury of the glenoid fossa played an important role in the genesis of TMJ ankylosis, and severe trauma to the glenoid fossa contributed to new bone formation in the joint space. Thirdly, fibrous ankylosis could be a suitable control for exploring the molecular pathogenesis of TMJ bony ankylosis.

Two questions arose: How does the severity of TMJ trauma impact the tissue differentiation in the joint space and lead to different outcomes — fibrous ankylosis or bony ankylosis? What is the cellular and molecular basis underlying the two conditions? One of the main histological features of TMJ bony ankylosis is a prolonged chondral phase compared with condylar fracture healing (Yan et al., 2013, 2014b), while fibrous ankylosis is characterized by abundance of fibrous tissue with a very small amount of cartilage or even no cartilage in the joint space (Yan et al., 2013). Similarly, delayed bone healing or hypertrophic nonunions have substantial callus that contains a lot of cartilage, while atrophic nonunions usually exhibit fibrous scar tissue with minimal callus or cartilage in the fracture gap (Peters et al., 2010; Kostenuik and Mirza, 2017). Therefore, we previously proposed a hypothesis that the genesis of TMJ ankylosis was a compromised bone healing course between the two injured articular surfaces under the effect of opening movement (Yan et al., 2012). In particular, TMJ bony ankylosis was similar to delayed bone healing or hypertrophic non-union (Yan et al., 2012, 2014a), and fibrous ankylosis was similar to atrophic non-union (Yan et al., 2014c).

Based on the hypothesis and the established animal model, we found that mRNA expression levels for several genes regulating bone formation, such as wingless-type MMTV integration site family, member 5A (Wnt5a), β-catenin, lymphoid enhancer binding factor 1 (Lef1), runt-related transcription factor 2 (Runx2), osterix, transcription factor SOX9 (Sox9), bone morphogenetic protein 2 (Bmp2), and bone morphogenetic protein 7 (Bmp7) in bony ankylosed callus were inclined to be higher than those in fibrous ankylosed callus (Yan et al., 2014a). These findings indicated that enhanced Wnt/β-catenin and Bmp signaling pathways contributed to new bone formation in the joint space and promoted the development of bony ankylosis.

Aside from growth factors/cytokines, blood vessel formation also plays a prominent role in bone healing. It is well known that an adequate blood supply is a prerequisite for successful bone healing (Hausman et al., 2001). Ischemia or local inhibition of angiogenesis will result in compromised fracture healing (Lu et al., 2007; Fassbender et al., 2011). Two main pathways regulate blood vessel formation during bone healing. One is a vascular endothelial growth factor (VEGF)-dependent pathway (Ai-Aql et al., 2008). VEGF is a specific mitogen for vascular endothelial cells. It is well known that VEGF signaling plays a key role in neo-angiogenesis and in endochondral bone formation (Ai-Aql et al., 2008). The VEGF family consists of at least six members: VEGF-A (VEGF), VEGF-B, VEGF-C, VEGF-D, VEGF-E and placental growth factor (Hu and Olsen, 2016). VEGF is commonly referred to as VEGF-A, because VEGF-A is the most abundant form. Five VEGF signaling receptors have been found to date. Kinase insert domain receptor (VEGFR2), as the major receptor transducing VEGF signaling, interacts with VEGF to mediate angiogenesis and promotion of vessel permeability (Ferrara et al., 2003). However, the functional significance of soluble vascular endothelial growth factor receptor-1 (VEGFR1) remains to be determined. VEGFR1 may serve as a decoy receptor to prevent VEGF from binding to VEGFR2, or it can function as a signaling receptor like VEGFR2 (Hu and Olsen, 2017).

A second pathway that regulates vascular growth is an angiopoietin-dependent pathway, which includes angiopoietin-1 (Ang 1), angiopoietin-2 (Ang 2), and their receptor, i.e. TEK receptor tyrosine kinase (Tie2) (Ai-Aql et al., 2008). Tie2 is a transmembrane tyrosine kinase whose expression is almost exclusive to the endothelium of blood vessels (Eklund et al., 2017). Ang1 is a canonical Tie2 agonist, which is made by and secreted from peri-endothelial cells and platelet α-granules (Parikh, 2017). Signaling by Ang1 promotes vascular endothelial cell survival and the sprouting and reorganization of blood vessels (Moss, 2013). Unlike the paracrine Ang1, Ang2 is expressed by epithelial cells and acts as an autocrine context-dependent agonist/antagonist of Tie2 (Eklund et al., 2017). Both Ang1 and Ang2 play crucial roles during fracture healing (Ai-Aql et al., 2008).

Besides VEGF and the Angs, other factors that stimulate blood vessel formation, and which have a broader target cell spectrum, include hypoxia inducible factor 1, alpha (HIF-1α), fibroblast growth factor 2 (FGF2), cysteine-rich protein 61 (CYR61), platelet/endothelial cell adhesion molecule 1 (CD31), matrix metallopeptidase 2 (MMP2), matrix metallopeptidase 9 (MMP9), and so on (Woodfin et al., 2007; Lienau et al., 2009; Riddle et al., 2009). HIF-1 comprises a hypoxia-inducible subunit HIF-1α and a constitutively expressed subunit HIF-1β, in which HIF-1α protein levels determine HIF-1 transcriptional activity. HIF-1α can interact with its transcriptional coactivators and further promote transcription of target genes involved in angiogenesis (Araldi and Schipani, 2010).

FGF2 possesses broad mitogenic and angiogenic activities. As an angiogenic growth factor, FGF2 induces endothelial cell proliferation and migration, and stimulates neovascularization (Presta et al., 2018). CYR61 is a matricellular protein that resides in the extracellular matrix, but serves regulatory rather than structural roles (Zhao et al., 2018). CYR61 modulates vascular formation through binding to the $\alpha_v\beta_3$ integrin to enhance endothelial cell adhesion, migration, proliferation, and microtubule formation, or indirectly by accommodating the activity of VEGF/VEGF receptors (Grote et al., 2007; Yu et al., 2008; Yang et al., 2018). CD31 is expressed in the vascular compartment, including endothelial cells, platelets, and leukocytes, and is identified as an endothelial cell junction molecule (Woodfin et al., 2007). CD31 plays an important role in angiogenesis through modulating endothelial cell migration, adhesion, and proliferation (Park et al., 2015). Proteins of the matrix metalloproteinase (MMP) family mediate the degradation of the extracellular matrix, which is a prerequisite for angiogenesis. Through cleaving the extracellular matrix, MMPs can initiate the migration of endothelial cells and the development of neovasculature (Deryugina and Quigley, 2015). Among MMPs, matrix metallopeptidase 2 (MMP2) is involved in intramembranous bone formation, while matrix metallopeptidase 9 (MMP9) plays a significant role during endochondral ossification (Lienau et al., 2009).

Angiogenesis and osteogenesis are closely integrated (Kusumbe et al., 2014; Grosso et al., 2017). Recent studies have shown that VEGF produced by osteoblast progenitor cells stimulate osteoblast differentiation via an intracrine mechanism (Liu et al., 2012; Berendsen and Olsen, 2014). Therefore, we hypothesized that angiogenesis affected the outcome of TMJ trauma, and that

increased neovascularization in the joint space after severe TMJ trauma promoted new bone formation in the joint space, ultimately resulting in bony ankylosis. The aim of this study was to compare the temporal expression pattern of several factors related to blood vessel formation during the development of TMJ fibrous and bony ankylosis, using our previously established ovine model. We hoped that the experimental findings would contribute to advancing the understanding of the molecular mechanisms involved in traumatic TMJ ankylosis.

2. Materials and methods

2.1. Animal model building and tissue harvesting

This study was approved by the ethics committees of Tianjin Stomatological Hospital (Tjskq2013001). 40 3-month-old male Xiaowei-Han sheep — a local strain — with an average preoperative weight of 23.5 ± 1.9 kg were used in this study. The housing and husbandry conditions of the animals, including bedding material, breeding programme, light/dark cycle, temperature, water quality, and food etc., were the same as previously described (Wang et al., 2018). Bilateral TMJ surgery was performed on each sheep. The surgical procedure for inducing TMJ ankylosis was similar to the previous study (Yan et al., 2013).

Briefly, condylar sagittal fracture, severe damage to the glenoid fossa, and removal of the lateral 2/3 disc were performed on the right joint (Fig. 1A–F), which had been shown to induce bony ankylosis at 6 months postoperatively via an intermediate stage of fibro-osseous ankylosis at 1 month and 3 months postoperatively (Yan et al., 2013). On the left TMJ, condylar sagittal fracture, minor damage to the glenoid fossa, and removal of the lateral 2/3 disc were performed (Fig. 1A–C, G and H), which had previously been shown to induce fibrous ankylosis at 3 months and 6 months after surgery (Yan et al., 2013).

Ten animals were sacrificed and tissue harvested from the bilateral TMJs at postoperative days 7, 14, 28, and 56 after surgery, respectively. At 2 time points, namely postoperative days 28 and 56, three animals were allocated to receive the examination of computed tomography (CT) before sacrifice. CT was taken at 120 kV, 130 mA, 1-s rotation time, and 2-mm slice thickness using a GE light-speed 16-slice CT scanner. Multiplanar reformation was used to generate coronal CT images of the TMJ. The bone window setting was selected for observation of the structures of TMJ. The morphological features of shape, erosion of the condylar and the temporal surfaces, and the calcification in the joint gap were identified.

For each time point of tissue harvesting, three out of 10 animals were sacrificed for histological analysis, and the other seven for ribonucleic acid (RNA) extraction. For histological analysis, the TMJ complexes were removed en bloc with a band saw and fixed in 10% natural buffered formalin (Yan et al., 2013). For RNA extraction, the TMJ complexes were carefully removed en bloc with a fissure bur and a wide osteotome, and then any soft tissue was promptly dissected from around the joint. The ankylosed joints were split open carefully using a narrow osteotome, and the newly generated tissue in the joint space, namely ankylosed callus, was harvested (Fig. 2). The ankylosed callus was rapidly frozen in liquid nitrogen and stored at −80 °C for RNA extraction.

2.2. Total RNA extraction and the synthesis of cDNA

The ankylosed callus was crushed using a mortar and pestle in liquid nitrogen. The total RNA was extracted from the lysate using Trizol reagent (Invitrogen, Carlsbad, USA) according to the manufacture's instructions. The concentration of each RNA sample was determined spectrophotometrically and the integrity of all RNA samples was monitored on denaturing agarose gel electrophoresis. Reverse transcription was performed with a cDNA synthesis kit (Promega, USA) in a 20 μl reaction system containing 4 μg total RNA (Yan et al., 2014a).

2.3. Primer design and the identity of products

Primers for each target gene were designed using Primer Premier software version 5.0. The primers were synthesized by Sangon Biotech (Shanghai) Co., Ltd. Before the quantitative real-time PCR, reverse transcription-PCR was carried out to verify the reliability of primers, using the total RNA isolated from the sheep bone or muscle. The PCR products were visualized on a 1.5% agarose gel stained with GoldenView™, using Gel Imaging System. When the amplified PCR products manifested as a single band, with a suitable abundance of expression and of a predicted size, by electrophoresis, they were sent to BGI Sequencing (Beijing) and sequenced in both directions. The bidirectional sequencing results were spliced and formed the full-length nucleotide sequences of the products. Then the sequences of the products and the template were compared by BLAST on PubMed. The two sequences were identified as the same gene when their homology was more than 95%. The bands of partial products are shown in Fig. 3. The primers for the target genes, confirmed by sequencing and BLAST, are shown in Table 1.

2.4. Real-time PCR

Real-time PCR analysis (LightCycler 480 II; Roche, Switzerland), using SYBR green, was performed to assess changes in gene expression. The reaction system and PCR cycle parameters were the same as previously described (Yan et al., 2014a). Relative gene expression was calculated using the $2^{-\Delta\Delta Ct}$ method. The housekeeping glyceraldehyde-3-phosphate dehydrogenase (GAPDH) gene was used for normalization of target gene expression, with the threshold cycle (C_T) values of the target gene from duplicate runs being averaged and calibrated in relation to GAPDH C_T values. The normalized level for the target gene was then compared with the target signals in the 7-day samples of fibrous ankylosed callus, which served as calibrator, using the comparative C_T method. Finally, the values for mRNA expression were compared between the fibrous and bony ankylosed callus.

2.5. Histology/immunohistochemistry

The TMJ complexes were decalcified with a mixture of 0.5% concentrated hydrochloric acid and 0.5% glacial acetic acid for 1 week, and then in buffered 19% ethylenediaminetetraacetic acid (EDTA) (pH 7.2–7.4) for 6 weeks at room temperature. The well-decalcified specimens were embedded in paraffin. 5-μm-thick sections were cut with a microtome, and the slides were examined after staining with hematoxylin and eosin. To further analyze angiogenesis in ankylosed callus, immunohistochemistry for alpha-smooth muscle actin was performed on the 7-, 14-, 28-, and 56-day tissue samples as follows. Deparaffinized and rehydrated sections were incubated in 10% normal horse serum to block non-specific binding. After blocking, the sections were incubated with a monoclonal anti-human antibody to alpha-smooth muscle actin (α-SMA) from mouse (1:50, Dako, Denmark). After washing, the sections were exposed to enzyme-labeled goat anti-rabbit IgG secondary antibody (ZSGB-BIO, Beijing, China), to detect the primary antibody. Horseradish peroxidase in the second antibody detection system catalyzed the reaction of substrate H_2O_2 with 3,3-diaminobenzidine tetrahydrochloride solution (1:20, ZSGB-BIO, Beijing, China) to form a brown, insoluble antigen-antibody

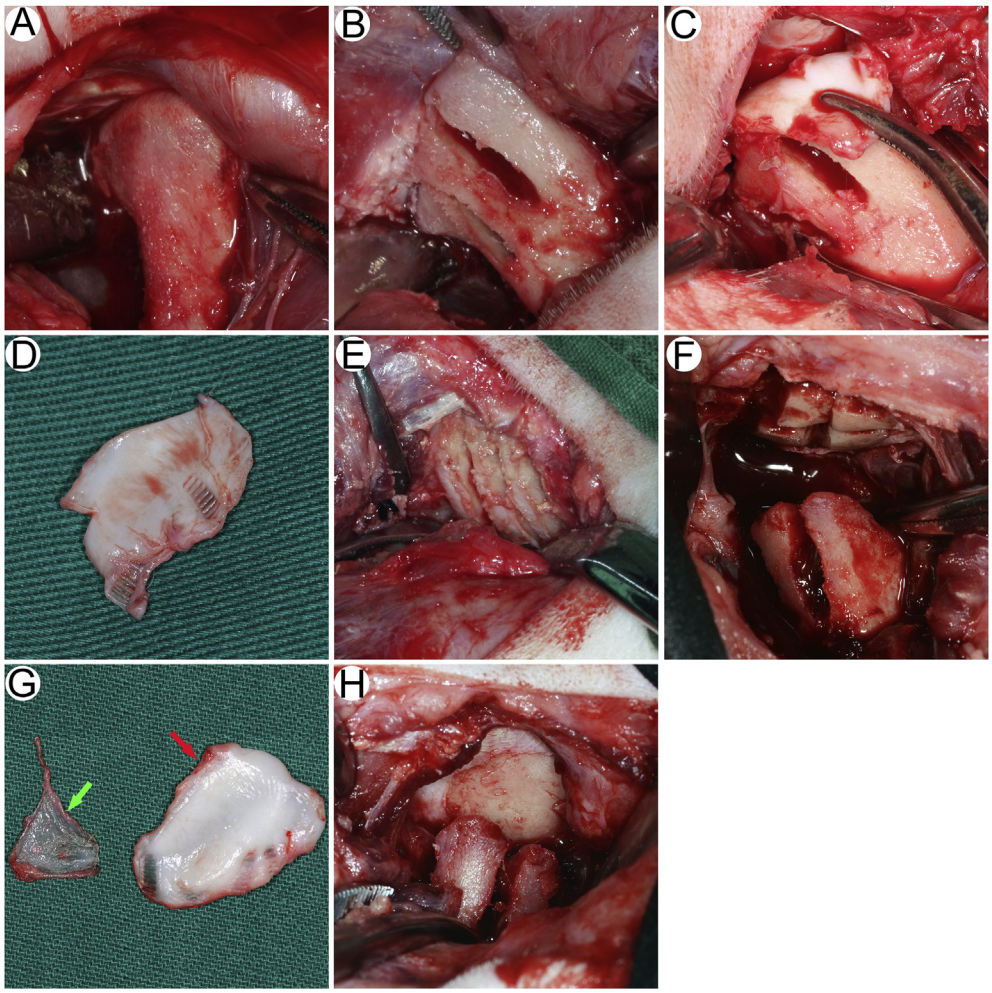

Fig. 1. Surgical procedures to build up fracture-induced TMJ ankylosis model. A, Exposure of the condyle; B, Two parallel deep grooves in sagittal plain divided the condyle into 3 bony pillars; C, Fracture of the medial pillars and exposure of the superior joint space and the disc; D, Excision of the lateral 2/3 disc; E and F, Severe trauma of the glenoid fossa for inducing bony ankylosis, i.e., Carving deep grooves in the glenoid fossa until the exposure of cancelous bone with bleeding; G and H, Minor trauma of the glenoid fossa for inducing fibrous ankylosis, i.e., removal of the fibrous layer covering on the glenoid fossa. H, the excised disk (red arrow) and the fibrous layer of the glenoid fossa (green arrow).

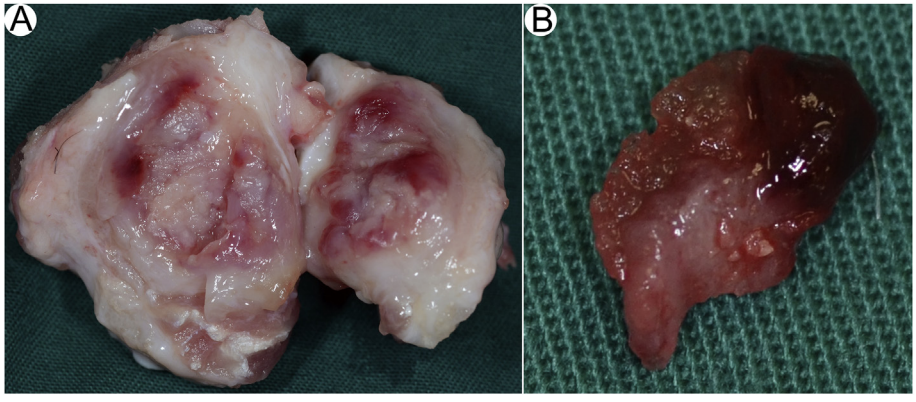

Fig. 2. The site of tissue harvesting: in A, the ankylosed joint was split open; in B, the callus in the joint space was removed for RNA extraction.

complex, which indicated a specific antigen site. Sections were counterstained with hematoxylin and dehydrated. Sections incubated without the primary antibody served as a negative control. No section showed any staining in this control experiment.

2.6. Statistical analyses

For statistical analyses of data, medians were calculated and statistical comparisons between fibrous and bony ankylosis callus for each time point were performed using the Wilcoxon signed-

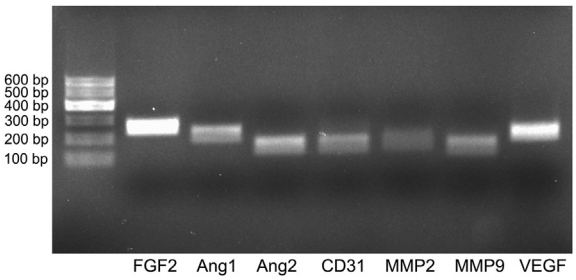

Fig. 3. PCR results for partial genes with single band, suitable level of expression, and predicted size.

rank test (SPSS 17.0). The level of statistical significance was taken as $p < 0.05$.

3. Results

3.1. Radiographic examination (Fig. 4)

The animals showed clear fracture line on the condyle, smooth surface of the glenoid fossa without intra-articular calcification in the fibrous ankylosis-inducing side at day 28 after operation (Fig. 4A). However, the glenoid fossa surface presented with an erosive feature and calcified callus image appeared in the joint space in the bony ankylosis-inducing side at day 28 after operation (Fig. 4A). The joints in the fibrous ankylosis-inducing side showed an irregular thickened feature of the glenoid fossa with no signs of intra-articular calcification 56 days postoperatively (Fig. 4B). However, extensive erosion of glenoid fossa surface with intra-articular calcification could be found in the bony ankylosis-inducing side at the same time (Fig. 4B).

3.2. Histological analysis

Histological analysis of the 7-day tissue samples from both fibrous ankylosed and bony ankylosed joints showed large amounts of granulation tissue, a fibrin scaffold, and a residual hematoma (Figs. 5A–C and 6A–C). The new blood vessels within the granulation tissue could be detected in the ankylosed callus by immunohistochemistry (Fig. 7A, B). A difference in histological appearance was seen in the 14-day tissue samples between the fibrous ankylosed and bony ankylosed joints (Figs. 5D–F and 6D–F). Although fibrous connective tissue occupied the joint space and no cartilage had formed at day 14 in both types of ankylosed joint, the distribution of the collagen in the fibrous ankylosed joints was more disorganized than that in the bony ankylosed joints (Figs. 5D–F and 6D–F). In addition, coarse collagen and remnants of the hematoma could be found in the fibrous ankylosed joints, but not in the bony ankylosed joints. The blank area without any tissue in the fibrous ankylosed joints was larger than that in the bony ankylosed joints (Figs. 5D–F and 6D–F). Immunohistochemical examination showed plenty of blood vessels in the fibrous connective tissue in both types of ankylosis (Fig. 7C and D).

At day 28, in the presence of a lot of fibrous tissue, cartilage had formed locally in the bony ankylosed joint space (Fig. 5G–I). In particular, multinuclear chondroclasts and neovascularization could be seen in the center of a cartilaginous scaffold, indicating late stages of endochondral ossification (Fig. 5H and I). In contrast, the fibrous ankylosed joint space was full of fibrous tissue without cartilage (Fig. 6 G–I). At day 56, the bony ankylosed joint space was composed of abundant cartilage cells, cartilage matrix, and a small amount of fibrous tissue, in which neoformative, mineralized, woven bone could be seen (Fig. 5J–L). More extensive endochondral formation and partial primary bone formation had occurred in

Table 1
Sequences of primers for real-time PCR.

Gene	GenBank accession no.	Sequence of forward and reverse primers	Annealing temperature	Product size
Ang1	XM_004011787.3	5′ GTGCCTACACTTTCATTC 3′ 5′ CCATCTCCGACTTCATA 3	50 °C	216 bp
Ang2	XM_004021671.3	5′ TGGGAAGAAACAGTATCAG 3′ 5′ ACCGAGTCGTCGTAGTC 3′	56 °C	144 bp
CD31	XM_004013029.3	5′ AGTTGAGGAGCAAGACCG 3′ 5′ GAAGGATTCCCGCACAG 3′	51 °C	118 bp
CYR61	XM_012175059.2	5′ CAGTGCTGTGAGGAGTGGGTC 3′ 5′ GGGTGTAAAGAATGCGAGGTT 3′	58 °C	202 bp
FGF2	NM_001009769.1	5′ GAGCGACCCTCACATCAA 3′ 5′ CGTTTCAGTGCCACATACC 3′	52 °C	222 bp
Hif-1α	XM_015097105.1	5′ TCTCCATTACCTGCCTCTG 3′ 5′ AACTTTGTCTGGTGCTTCC 3′	52 °C	178 bp
MMP2	NM_001166180.1	5′ AACGCCATCCCTGATAACC 3′ 5′ TTCCGAACTTCACGCTCTT 3′	55 °C	124 bp
MMP9	XM_004014614.3	5′ CCCATTAGCACGCACGAC 3′ 5′ AGCCCACATAGTCCACCTGA 3′	54 °C	115 bp
SDF1	XM_012105583.1	5′ CCTTGCCGATTCTTTGAG 3′ 5′ AGTGGGACTGGGTTTGTTT 3′	52 °C	189 bp
TIE2	XM_012127828.2	5′ TCTGTGAAGGGCGAGTT 3′ 5′ GGCACCGAGTGGATGAA 3′	52 °C	196 bp
TIMP1	NM_001009319.2	5′ CCAGAATCGCAGTGAGGAG 3′ 5′ GGGATAGATGAGCAGGGAAAC 3′	56 °C	180 bp
VEGF	XM_012100430.2	5′ ATTGAGACCCTGGTGGA 3′ 5′ CCTATGTGCTGGCTTTG 3′	52 °C	191 bp
VEGFR2	XM_012179355.2	5′ GATGGGAACCGAAACCTA 3′ 5′ TCCTGGGCACCTTCTACT 3′	54 °C	128 bp
vWF	XM_012176134.2	5′ CCAAGGCTTTCATCTCAA 3′ 5′ GGGTCCACAAGGCTCA 3′	55 °C	139 bp
GAPDH	AF030943.1	5′ GCAAGTTCCACGGCACAG 3′ 5′ GGTTCACGCCCATCACAA 3′	58 °C	249 bp

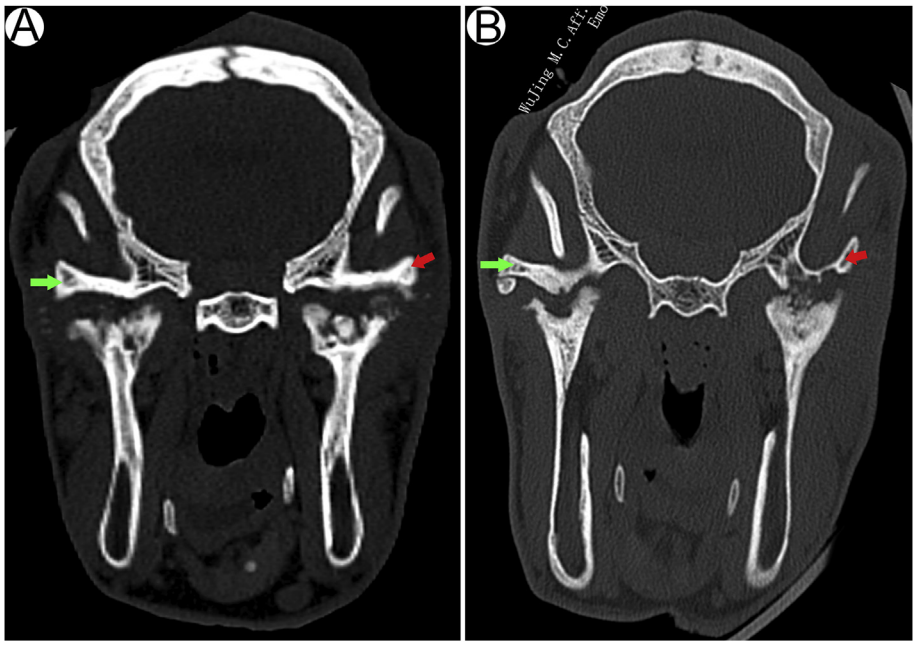

Fig. 4. The coronal CT manifests of the TMJ after surgery. A, the sagittal fracture lines in the bilateral condyles were still clear 28 days after operation. In the fibrous ankylosis-inducing side (green arrow), smooth surface of the glenoid fossa without intra-articular calcification could be found. In the bony ankylosis-inducing side (red arrow), the glenoid fossa surface showed an erosive feature and calcified callus image appeared in the joint space. B, the sagittal fracture line in the bilateral condyles disappeared with an erosive feature on the surfaces of the condyles 56 days postoperatively. In the fibrous ankylosis-inducing side (green arrow), the glenoid fossa showed an irregular thickened feature with no signs of intra-articular calcification. In the bony ankylosis-inducing side, extensive erosion of glenoid fossa surface with intra-articular calcification could be found.

the bony ankylosis joint space compared with the histological appearance at day 28 (Fig. 5J–L). In contrast, large amount of fibrous tissue occupied the fibrous ankylosed joint space; however, no cartilage or osteogenesis could be seen (Fig. 6J–L). At days 28 and 56, new blood vessels could be seen in the fibrous tissue around the cartilage in the bony ankylosed joint space. The number of new blood vessels seemed lower in the fibrous ankylosed callus than in the bony ankylosed callus; however, immunohistochemistry revealed more vessels with a greater diameter in the former (Fig. 7E–H).

3.3. Real-time quantitative PCR

3.3.1. HIF-1α, VEGF, VEGFR2, and SDF1 (Fig. 8)

The expression levels of HIF-1α in bony ankylosis increased from day 7 to day 14, followed by a sustained expression from day 28 to day 56. In contrast, HIF-1α expression in fibrous ankylosis decreased from day 7 to day 14, followed by a continuous increase. Bony ankylosis showed a significantly higher HIF-1α expression at day 14 ($p = 0.003$) compared with fibrous ankylosis. Expression levels of VEGF peaked at day 14 in bony ankylosis, and at day 28 in fibrous ankylosis. Fibrous ankylosis showed significantly lower VEGF expression at day 7 ($p = 0.035$), day 14 ($p = 0.002$), and day 56 ($p = 0.006$). Regarding the expression of VEGFR2, no obvious change was found in bony ankylosis during the course of healing, while VEGFR2 expression in fibrous ankylosis peaked at day 28. Significantly higher values for VEGFR2 expression were found at day 7 ($p = 0.001$) in bony ankylosis. In both fibrous and bony ankylosis, the expression of SDF1 peaked at day 28. Gene expression of SDF1 was significantly higher in bony ankylosis from day 7 ($p = 0.001$) to day 14 ($p = 0.001$).

3.3.2. Ang1, Ang2, Tie2, and CD31 (Fig. 9)

Expression levels of Ang1 peaked at day 14 in bony ankylosis, and at day 28 in fibrous ankylosis. Gene expression of Ang1 was significantly lower from day 7 ($p = 0.004$) to day 14 ($p = 0.001$) in fibrous ankylosis. The expression of Ang2 in fibrous ankylosis peaked at day 28, while in bony ankylosis it showed a decreased expression at day 28 and an increased expression with a maximum value at day 56. Gene expression of Ang2 was significantly lower in fibrous ankylosis at day 7 ($p = 0.029$), while at day 28 it was significantly higher ($p = 0.024$). The expression of Tie2 peaked at day 14 in bony ankylosis, while in fibrous ankylosis there was increased expression at day 28 and a steady expression at day 56. At day 14, there was a significantly lower Tie2 expression in fibrous ankylosis ($p = 0.004$). The expression of CD31 peaked at day 14 in bony ankylosis, and at day 28 in fibrous ankylosis. The expression of CD31 was significantly higher in bony ankylosis from day 7 ($p = 0.008$) to day 14 ($p = 0.01$), while at day 28 it was significantly lower ($p = 0.003$).

3.3.3. vWF, CYR61, FGF2, and TIMP1 (Fig. 10)

The expression of von Willebrand factor (vWF), an endothelial cell marker, peaked at day 14 in bony ankylosis and at day 28 in fibrous ankylosis. Expression of vWF was significantly higher in bony ankylosis at day 14 ($p = 0.003$). CYR61 expression in bony ankylosis decreased from day 7 to day 14, and increased continuously to a maximum value at day 56. On the other hand, expression of CYR61 in fibrous ankylosis increased until day 56. Gene expression of CYR61 was significantly lower in fibrous ankylosis at day 7 ($p = 0.003$), day 14 ($p = 0.017$), and day 28 ($p = 0.001$). Expression of FGF2 in bony ankylosis increased continuously from day 7 to day 28, reaching a sustained level at day 56, while fibrous ankylosis showed a steady expression from day 7 to day 14, before increasing continuously to a maximum value at day 56. Gene expression of FGF2 was significantly lower in fibrous ankylosis from day 14 ($p = 0.008$) to day 28 ($p = 0.017$). Expression of TIMP1 peaked at day 14 in bony ankylosis, while in fibrous ankylosis there was no obvious change in expression over the course of healing.

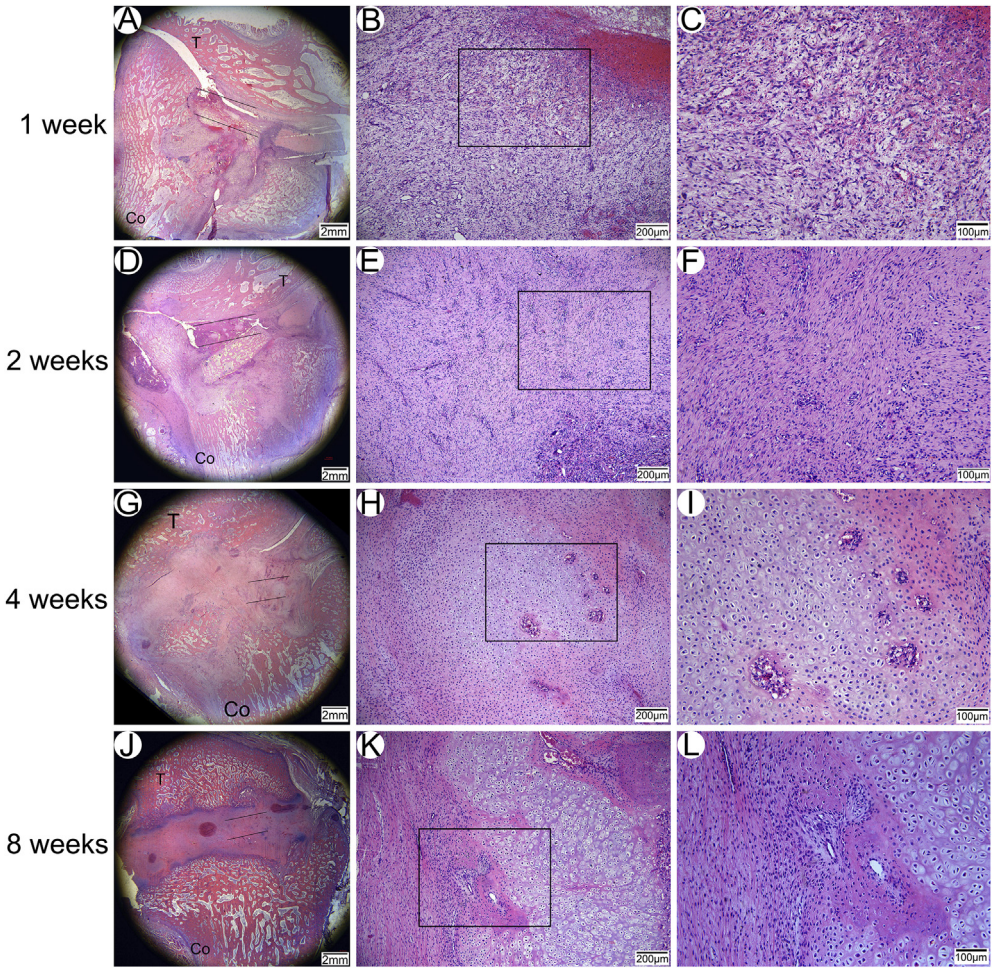

Fig. 5. Photomicrographs of histological sections from the bony ankylosis-induced side. (A–C) Granulation tissue with hematoma remnants at day 7 after surgery. (D–F) Fibrous connective tissue without cartilage in the joint space at day 14 after surgery. (G–I) Cartilage had formed and chondroclasts and neovascularization could be seen in the cartilaginous scaffold at day 28 after surgery. (J–L) Cartilage cells, cartilage matrix, and neoformative mineralized woven bone could be found at day 56 after surgery. (Hematoxylin and eosin stain. A, D, G, and J: magnification ×1.25; scale bar 2 mm. B, E, H, and K: magnification ×10; scale bar 200 μm. C, F, I, and L, magnification ×20; scale bar 100 μm)

Gene expression of TIMP1 was significantly lower in fibrous ankylosis at day 14 ($p = 0.001$).

3.3.4. *MMP2 and MMP9 (Fig. 11)*

The expression of MMP2 peaked at day 28 in bony ankylosis, while in fibrous ankylosis it showed a continuous increase over the whole healing period. Gene expression of MMP2 was significantly lower in fibrous ankylosis from day 14 ($p = 0.003$) to day 28 ($p = 0.006$). From day 7 to day 28, expression of MMP9 in both fibrous and bony ankylosis remained steady. However, an obvious increase was found in bony ankylosis at day 56 in contrast to a slight decrease in fibrous ankylosis. Expression of MMP9 was significantly lower in fibrous ankylosis from day 7 ($p = 0.002$) to day 14 ($p = 0.001$).

4. Discussion

One of the important goals of the treatment of TMJ ankylosis is to maintain normal mouth opening. Patients with bony ankylosis have more restricted mouth opening than those with fibrous ankylosis (Zhang et al., 2006; Yan et al., 2014c). In addition, the surgical management of bony ankylosis is more complicated than that for fibrous ankylosis (Sawhney, 1986; Long et al., 2005; Zhang and He, 2006), with the outcome of the former more uncertain than for the latter. According to our animal studies, hemarthrosis will inevitably develop into TMJ ankylosis as long as the physical barriers, including the disc and the articular fibrous layers, are damaged (Wang et al., 2018, 2019). Once the traumatic microenvironment for ankylosis is established, the outcome, whether fibrous or bony ankylosis, depends on the severity of the primary TMJ trauma (Cheung et al., 2007; Yan et al., 2013; Wang et al., 2018). This suggests two possible ways of preventing the occurrence of bony ankylosis. One is to eliminate the inducing conditions, for example by repositioning the displaced disc through surgical operation shortly after TMJ trauma. The other is to convert bony ankylosis into fibrous ankylosis, which largely depends on advancing understanding of the molecular mechanisms involved in the two types of TMJ ankylosis.

For our study, we chose an experimentally bilateral TMJ trauma model for comparative analysis. The histological outcomes demonstrated that fibro-osseous ankylosis, an intermediate stage of bony ankylosis, was achieved in the bony ankylosis-induced side and complete fibrous ankylosis was achieved in the fibrous ankylosis-induced side at 4 weeks and 8 weeks after surgery, verifying the repeatability of the animal model reported by our previous study (Yan et al., 2013). In addition, the early histological features of ankylosis in the animal model at 1 week and 2 weeks postoperatively were first shown in the present study. We found a

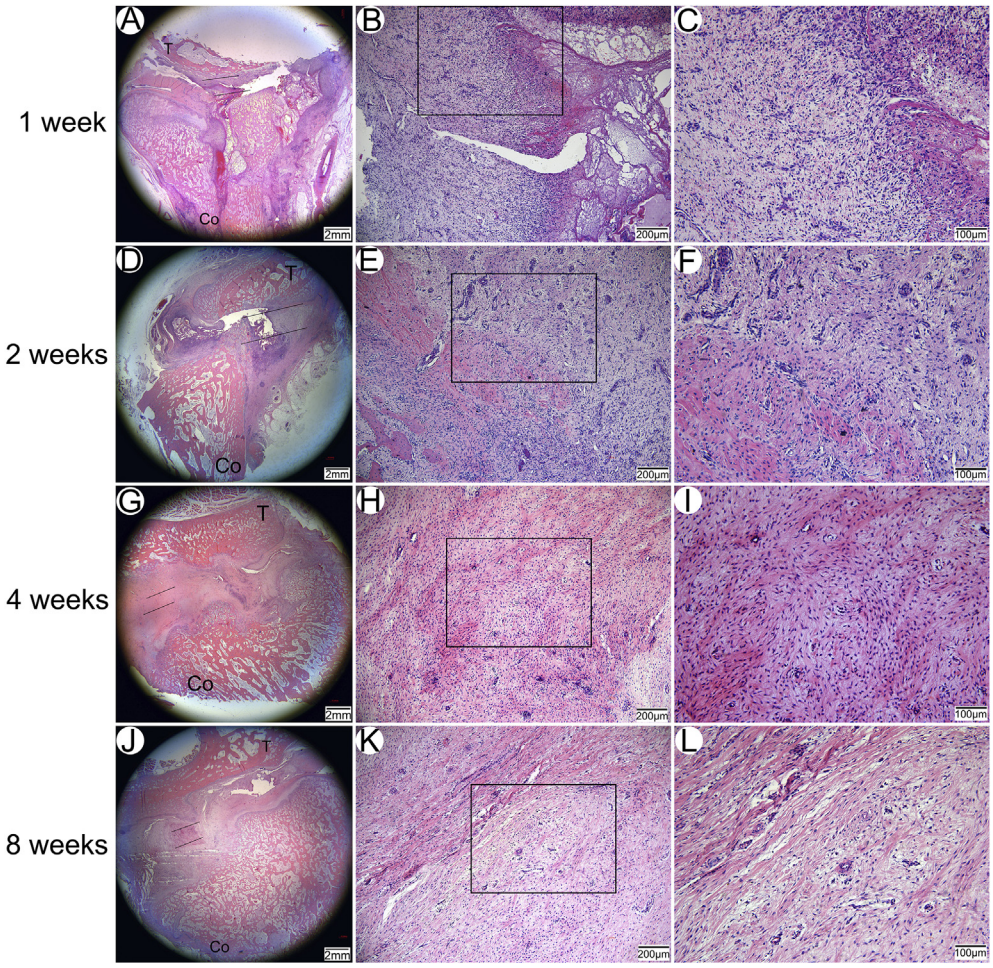

Fig. 6. Photomicrographs of histological sections from the fibrous ankylosis-induced side. (A–C) Granulation tissue with hematoma remnants at day 7 after surgery. (D–F) Fibrous connective tissue and remnants of the hematoma at day 14 after surgery. (G–I) Abundance of fibrous tissue without cartilage in the joint space at day 28 after surgery. (J–L) Mature fibrous tissue without cartilage in the joint space at day 56 after surgery. (Hematoxylin and eosin stain. A, D, G, and J: magnification ×1.25; scale bar 2 mm. B, E, H, and K: magnification ×10; scale bar 200 ìm. C, F, I, and L, magnification ×20; scale bar 100 μm)

prolonged presence of hematoma during the development of fibrous ankylosis, but not so for bony ankylosis. A larger blank area without any tissue in the fibrous ankylosed joints indicated a greater extent of hematoma absorption during the early development of fibrous ankylosis.

In this study, paired-sample Wilcoxon signed-rank tests were used to assess differences between individuals in this self-control-designed experiment. The temporal expression of molecules related to blood vessel formation was compared between fibrous ankylosis and bony ankylosis. These factors represented a broad spectrum of molecules acting directly and indirectly on endothelial cells, or relating to the remodeling of the extracellular matrix (Lienau et al., 2009). Among them, vWF, as an endothelial cell marker, was selected to indirectly evaluate the vascular state of the regenerative tissue (Lienau et al., 2009). The different temporal expression patterns for each investigated factor were established. More importantly, for the first time we could also show differential regulation of blood vessel formation between fibrous and bony ankylosis. Compared with bony ankylosis, fibrous ankylosis showed a delayed up-regulation in gene expression of HIF-1α, VEGF, SDF1, Ang1, Tie2, CD31, vWF, CYR61, FGF2, and MMP2. In addition, mRNA expression levels of HIF-1α, VEGF, VEGFR2, SDF1, Ang1, Tie2, vWF, CYR61, FGF2, TIMP1, MMP2, and MMP9 were distinctly lower in fibrous ankylosis compared with bony ankylosis at several time points. These results indicated delayed angiogenesis in fibrous ankylosis at the early stage and enhanced angiogenesis during the development of bony ankylosis.

It was assumed that the differential regulation of blood vessel formation was related to tissue differentiation in the joint space in the animal model. During the early stage of healing of TMJ trauma, five factors — VEGF, Ang1, Tie2, CD31, and vWF — peaked at day 14 in the bony ankylosis-induced side, but peaked at day 28 in the fibrous ankylosis-induced side, indicating delayed angiogenesis in fibrous ankylosis. In addition, the expressions of these five factors at day 14 were significantly higher in bony ankylosis than in fibrous ankylosis. Histological results at day 28 showed cartilage formation in bony ankylosis, in contrast to fibrous tissue presenting in the fibrous side. Therefore, the interval between days 14 and 28 was the key period for determining the organization of hematoma for the formation of either fibrous tissue or cartilage.

We believed that the enhanced angiogenesis at day 14 might be involved in determining chondrocyte differentiation and promoting the development of bony ankylosis. Our result was in accordance with previous studies. Angiogenesis was involved in tissue differentiation at the fracture site at the early stage of fracture healing (Street et al., 2002). Enhanced angiogenesis promoted chondrocyte differentiation at the fracture site (Lu et al., 2011); however, disturbed blood supply led to a significant reduction in

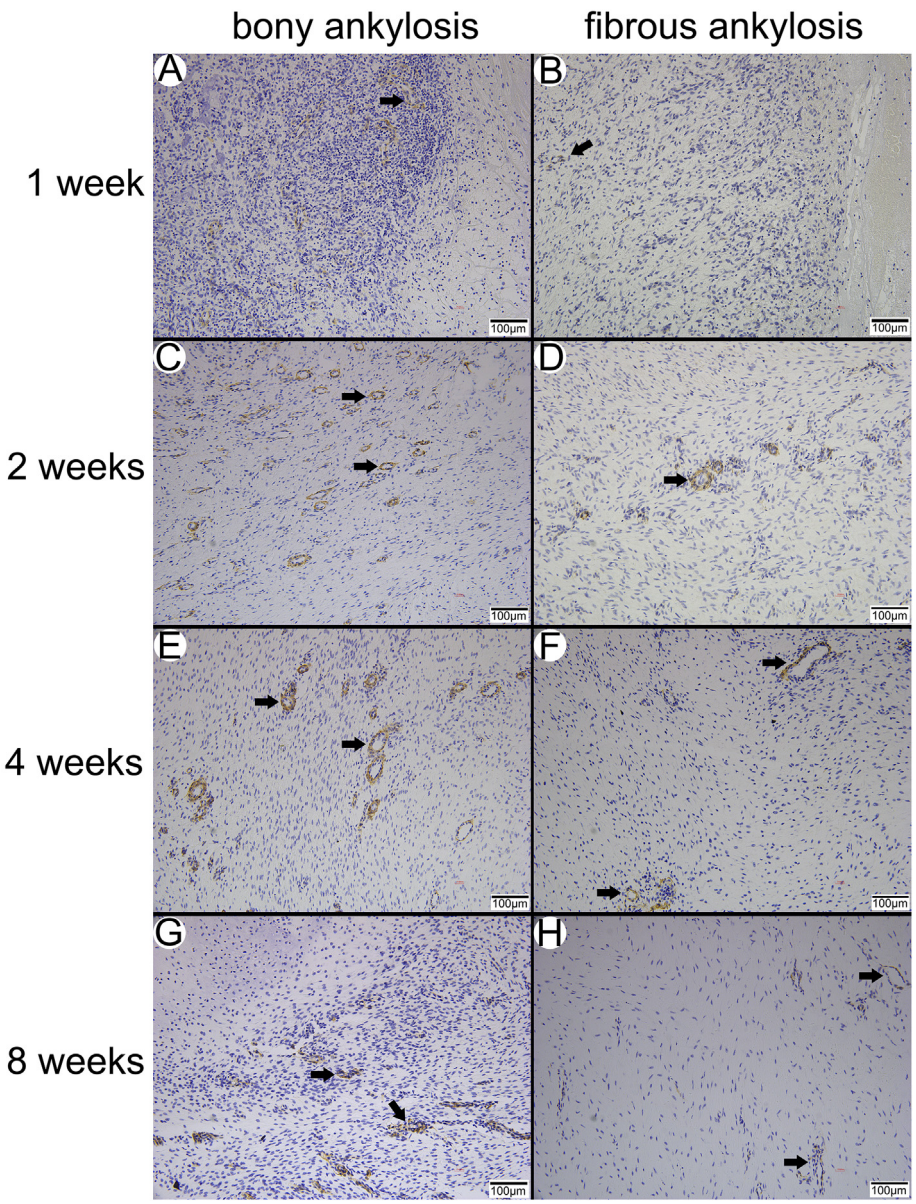

Fig. 7. Expression of alpha-smooth muscle actin (α-SMA) in fibrous and bony ankylosed callus. The arrows indicate blood vessels stained positive for α-SMA. (Immunohistochemistry stain. Magnification ×20; scale bar 100 μm)

cartilage and bone formation, ultimately resulting in atrophic nonunion (Lu et al., 2007; Oetgen et al., 2008; Fassbender et al., 2011). We thought a similar mechanism might be involved in determining the outcome — whether fibrous ankylosis or bony ankylosis — after TMJ trauma. In addition, the expression of CD31 and Ang2 was significantly higher in fibrous ankylosis than in bony ankylosis at day 28, indicating revascularization at the late stage of fibrous ankylosis. However, the critical window period for new bone formation had been missed (Brownlow et al., 2002), indicating the particularly important role of angiogenesis during the early stage of bony ankylosis.

Angiogenesis and osteogenesis are closely integrated. Previous studies have identified HIF-1α and the downstream target gene VEGF as the key molecular players in angiogenic-osteogenic coupling (Schipani et al., 2009; Maes et al., 2012). Osteoblast precursors were shown to move into the fracture site along with invading blood vessels, suggesting that blood vessels might have a role in determining the site of bone formation by carrying osteoprogenitors or mesenchymal stem cells (Maes et al., 2010).

As the initial stage of fracture healing, characterized by inflammation and hypoxia (Kolar et al., 2011), hematomas contain mesenchymal stem cells (Oe et al., 2007). In hypoxic conditions, the HIF-1α protein is stabilized and drives the inflammatory cells and mesenchymal stem cells to express the target gene VEGF (Hankenson et al., 2011). Then, bone marrow-derived endothelial progenitor cells are induced into circulatory system by VEGF and recruited into the fracture site via peripheral blood and differentiate into endothelial cells, ultimately promoting neo-angiogenesis (Lee et al., 2008; Matsumoto et al., 2008). On the other hand, the HIF-1α protein can recruit mesenchymal stem cells into the fracture site by regulating the expression of SDF1 (Kitaori et al., 2009; Liu et al., 2013). The mesenchymal stem cells are induced by HIF-1α protein to differentiate into chondrocytes at the fracture site (Robins et al., 2005).

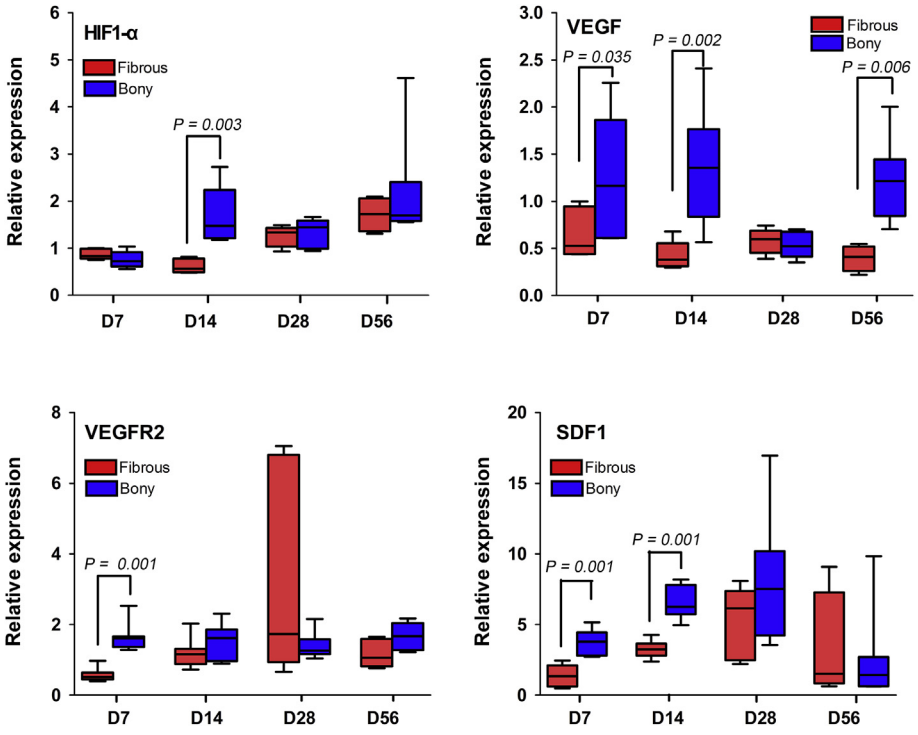

Fig. 8. Temporal gene expression of HIF1-α, VEGF, VEGFR2, and SDF1 in both fibrous and bony ankylosis. Results were normalized to GAPDH levels and compared with the target signals in the fibrous ankylosis on day 7, using the comparative Ct-method. Where given, the *p*-values show statistically significant differences between the fibrous and bony ankylosis at the indicated time point.

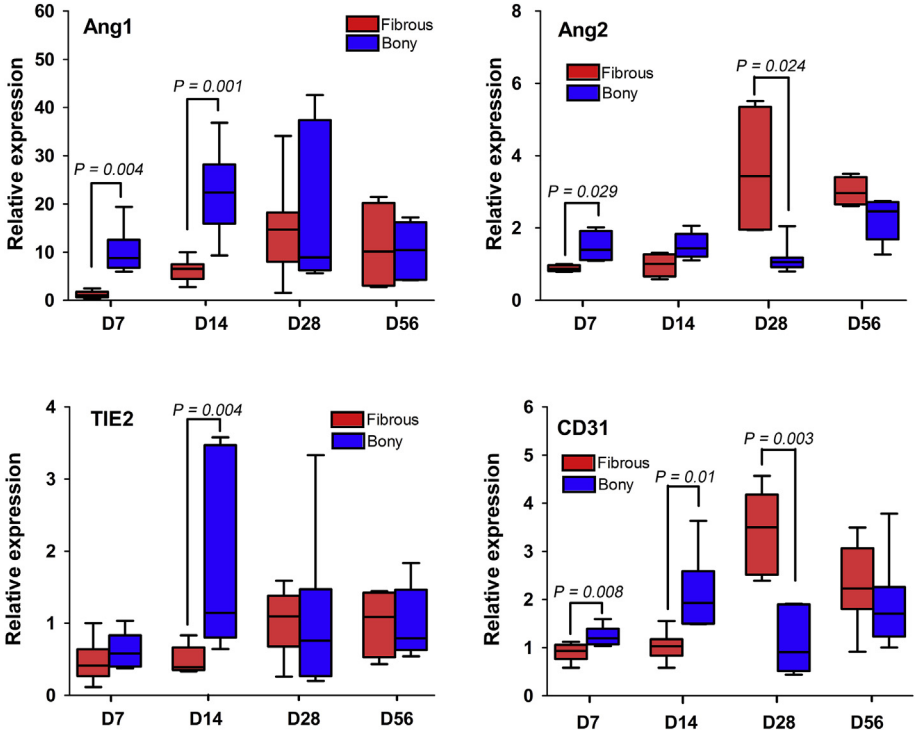

Fig. 9. Temporal gene expression of Ang1, Ang2, TIE2, and CD31 in both fibrous and bony ankylosis. Results were normalized to GAPDH levels and compared with the target signals in the fibrous ankylosis on day 7 using the comparative Ct-method. Where given, the *p*-values show statistically significant differences between the fibrous and bony ankylosis at the indicated time point.

In our study, the delayed up-regulation and lower expression of HIF-1α in fibrous ankylosis indicated more severe hypoxia in the hematomas of bony ankylosis. In the traumatic microenvironment inducing bony ankylosis, prolyl hydroxylation was inhibited and more HIF-1α protein accumulated due to the hypoxic conditions (Riddle et al., 2009). More HIF-1α induced a higher expression of

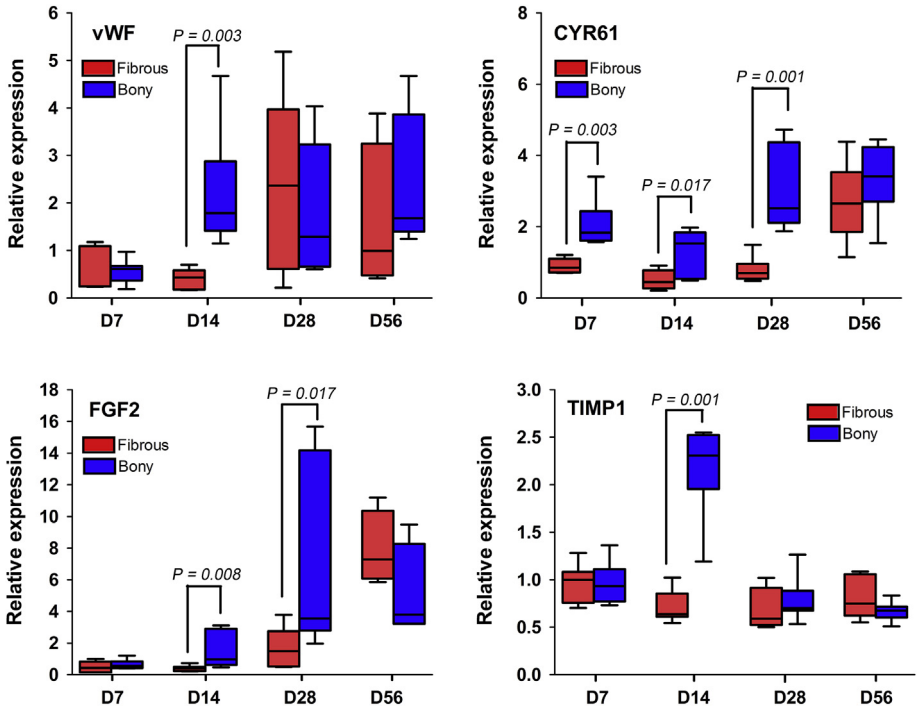

Fig. 10. Temporal gene expression of vWF, CYR61, FGF2, and TIMP1 in both fibrous and bony ankylosis. Results were normalized to GAPDH levels and compared with the target signals in the fibrous ankylosis on day 7 using the comparative Ct-method. Where given, the *p*-values show statistically significant differences between the fibrous and bony ankylosis at the indicated time point.

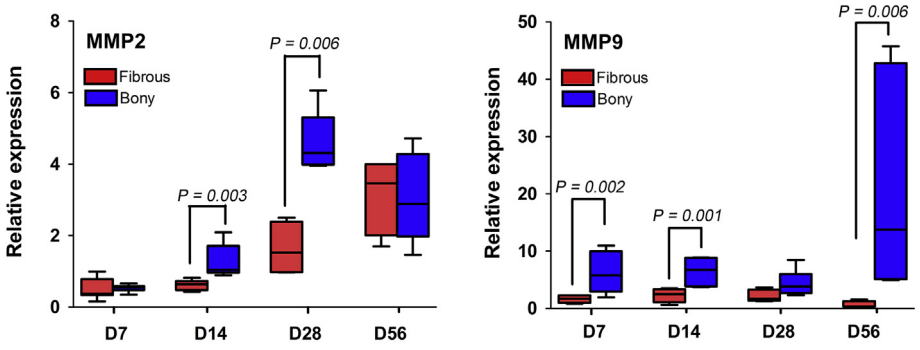

Fig. 11. Temporal gene expression of MMP2 and MMP9 in both fibrous and bony ankylosis. Results were normalized to GAPDH levels and compared with the target signals in the fibrous ankylosis on day 7 using the comparative Ct-method. Where given, the *p*-values show statistically significant differences between the fibrous and bony ankylosis at the indicated time point.

VEGF and other angiogenic factors, recruiting more vascular endothelial precursor cells from bone marrow into the TMJ joint space and promoting neo-angiogenesis. The new blood vessels not only maintained oxygen homeostasis, delivered nutrients, and removed waste, but also provided key signaling molecules to induce mesenchymal stem cells to differentiate into osteoblasts and chondroblasts, for example via the Wnt/β-catenin and Bmp signaling pathways (Yan et al., 2014b and 2014a). In addition, higher expression of SDF1 in the bony ankylosis-induced side indicated that more mesenchymal stem cells were recruited into the traumatic joint space. Therefore, cartilage and new bone formed in the joint space and bony ankylosis occurred. On the other hand, fibrous ankylosis developed because of the delayed angiogenesis and deficiency of key angiogenic factors in the milder TMJ traumatic microenvironment.

From another perspective, the differential gene expressions of angiogenic factors between fibrous and bony ankylosis might be not the 'cause', but simply the 'symptom' of differentiation under initially different traumatic microenvironments. In the sheep model, bilateral TMJ surgery was performed and more severe trauma was created on the bony ankylosis-induced side. Therefore, in chewing their food the animals might have relied on the joint that underwent milder trauma and limited motion in the joint receiving more severe trauma due to the pain and swelling, especially in the early stages after surgery. In other words, the mechanical environment might be more unstable on the fibrous ankylosis-induced side than on the bony ankylosis-induced side. The initial phase of fracture healing and the early vascular response are specifically sensitive to mechanical conditions (Klein et al., 2003). It is well accepted that mechanical instability during fracture healing can lead to an inhibition of vascularization (Lienau et al., 2005). Larger axial or shear movements can lead to a smaller number of vessels in the bone healing area than with smaller corresponding movements (Claes et al., 2002; Lienau et al.,

2005). In our study, remnants of the hematoma in the fibrous ankylosis-induced joint remained present for longer than in the bony ankylosis-induced joint, indicating that newly formed blood vessels might have ruptured due to larger tissue strains in the former, which was in accordance with previous studies (Epari et al., 2006; Lienau et al., 2009).

There are several limitations to the study results that need to be considered. First, the differential gene expression patterns we identified were specific to our induced fibrous and bony ankylosis model in sheep. As already mentioned, no animal model exactly mimics human disease, so our results cannot necessarily be generalized to TMJ ankylosis in human beings. However, specimens from patients with TMJ fibrous ankylosis have shown avascular, dense, fibrous tissue in the joint space (Blackwood, 1957; Li et al., 2014), whereas bony ankylosis cases have demonstrated abundant angiogenesis associated with endochondral ossification (Li et al., 2014). Second, given the presence of these differences in gene expression, it does not mean that the expression of the gene products also undergoes the same changes, so methods of quantitative protein analysis should be applied to verify the differences in expression of interesting proteins. Third, except for the Ang/Tie system being largely endothelial-cell specific, other factors exert additional effects not directly related to blood vessel formation. For instance, HIF1-α and CYR61 also promote chondrogenic differentiation (Robins et al., 2005; Schipani et al., 2009). Last but not least, we only studied four specific time points during the healing course of TMJ trauma. Ideally, more time points should be selected to show the temporal patterns of gene expression more precisely.

5. Conclusion

Our study, for the first time, demonstrated a differential regulation of blood vessel formation between fibrous and bony ankylosis in a sheep TMJ trauma model. Furthermore, this study provided evidence for our hypothesis that angiogenesis impacts tissue differentiation in the joint space, and enhanced angiogenesis, especially in the early stages, promotes the development of bony ankylosis after severe TMJ trauma. These results indicate that inhibition of angiogenesis in the joint space after TMJ trauma might be a promising strategy for preventing bony ankylosis in the future.

Conflicts of interest

The authors declare no conflicts of interest.

Disclosures

This investigation was supported by the National Natural Science Foundation of China (81300901), the Natural Science Foundation of Tianjin City, China (14JCQNJC12500) and the Key Clinical Program of Tianjin City on Oral and Maxillofacial Surgery.

Acknowledgments

None.

Appendix A. Supplementary data

Supplementary data to this article can be found online at https://doi.org/10.1016/j.jcms.2019.07.032.

References

Ai-Aql ZS, Alagl AS, Graves DT, Gerstenfeld LC, Einhorn TA: Molecular mechanisms controlling bone formation during fracture healing and distraction osteogenesis. J Dent Res 87: 107–118, 2008
Araldi E, Schipani E: Hypoxia, HIFs and bone development. Bone 47: 190–196, 2010
Berendsen AD, Olsen BR: How vascular endothelial growth factor-A (VEGF) regulates differentiation of mesenchymal stem cells. J Histochem Cytochem 62: 103–108, 2014
Blackwood HJ: Intra-articular fibrous ankylosis of the temporomandibular joint. Oral Surg Oral Med Oral Pathol 10: 634–642, 1957
Brownlow HC, Reed A, Simpson AH: The vascularity of atrophic non-unions. Injury 33: 145–150, 2002
Cheung LK, Shi XJ, Zheng LW: Surgical induction of temporomandibular joint ankylosis: an animal model. J Oral Maxillofac Surg 65: 993–1004, 2007
Claes L, Eckert-Hubner K, Augat P: The effect of mechanical stability on local vascularization and tissue differentiation in callus healing. J Orthop Res 20: 1099–1105, 2002
Deryugina EI, Quigley JP: Tumor angiogenesis: MMP-mediated induction of intravasation- and metastasis-sustaining neovasculature. Matrix Biol 44–46: 94–112, 2015
Eklund L, Kangas J, Saharinen P: Angiopoietin-Tie signalling in the cardiovascular and lymphatic systems. Clin Sci (Lond) 131: 87–103, 2017
Epari DR, Schell H, Bail HJ, Duda GN: Instability prolongs the chondral phase during bone healing in sheep. Bone 38: 864–870, 2006
Fassbender M, Strobel C, Rauhe JS, Bergmann C, Schmidmaier G, Wildemann B: Local inhibition of angiogenesis results in an atrophic non-union in a rat osteotomy model. Eur Cell Mater 22: 1–11, 2011
Ferrara N, Gerber HP, LeCouter J: The biology of VEGF and its receptors. Nat Med 9: 669–676, 2003
Grosso A, Burger MG, Lunger A, Schaefer DJ, Banfi A, Di Maggio N: It takes two to tango: coupling of angiogenesis and osteogenesis for bone regeneration. Front Bioeng Biotechnol 5: 68, 2017
Grote K, Salguero G, Ballmaier M, Dangers M, Drexler H, Schieffer B: The angiogenic factor CCN1 promotes adhesion and migration of circulating CD34+ progenitor cells: potential role in angiogenesis and endothelial regeneration. Blood 110: 877–885, 2007
Hankenson KD, Dishowitz M, Gray C, Schenker M: Angiogenesis in bone regeneration. Injury 42: 556–561, 2011
Hausman MR, Schaffler MB, Majeska RJ: Prevention of fracture healing in rats by an inhibitor of angiogenesis. Bone 29: 560–564, 2001
He LH, Xiao E, Duan DH, Gan YH, Zhang Y: Osteoclast deficiency contributes to temporomandibular joint ankylosed bone mass formation. J Dent Res 94: 1392–1400, 2015
Hu K, Olsen BR: The roles of vascular endothelial growth factor in bone repair and regeneration. Bone 91: 30–38, 2016
Hu K, Olsen BR: Vascular endothelial growth factor control mechanisms in skeletal growth and repair. Dev Dyn 246: 227–234, 2017
Kitaori T, Ito H, Schwarz EM, Tsutsumi R, Yoshitomi H, Oishi S, et al: Stromal cell-derived factor 1/CXCR4 signaling is critical for the recruitment of mesenchymal stem cells to the fracture site during skeletal repair in a mouse model. Arthritis Rheum 60: 813–823, 2009
Klein P, Schell H, Streitparth F, Heller M, Kassi JP, Kandziora F, et al: The initial phase of fracture healing is specifically sensitive to mechanical conditions. J Orthop Res 21: 662–669, 2003
Kolar P, Gaber T, Perka C, Duda GN, Buttgereit F: Human early fracture hematoma is characterized by inflammation and hypoxia. Clin Orthop Relat Res 469: 3118–3126, 2011
Kostenuik P, Mirza FM: Fracture healing physiology and the quest for therapies for delayed healing and nonunion. J Orthop Res 35: 213–223, 2017
Kusumbe AP, Ramasamy SK, Adams RH: Coupling of angiogenesis and osteogenesis by a specific vessel subtype in bone. Nature 507: 323–328, 2014
Laskin DM: Role of the meniscus in the etiology of posttraumatic temporomandibular joint ankylosis. Int J Oral Surg 7: 340–345, 1978
Lee DY, Cho TJ, Kim JA, Lee HR, Yoo WJ, Chung CY, et al: Mobilization of endothelial progenitor cells in fracture healing and distraction osteogenesis. Bone 42: 932–941, 2008
Li JM, An JG, Wang X, Yan YB, Xiao E, He Y, et al: Imaging and histologic features of traumatic temporomandibular joint ankylosis. Oral Surg Oral Med Oral Pathol Oral Radiol 118: 330–337, 2014
Lienau J, Schell H, Duda GN, Seebeck P, Muchow S, Bail HJ: Initial vascularization and tissue differentiation are influenced by fixation stability. J Orthop Res 23: 639–645, 2005
Lienau J, Schmidt-Bleek K, Peters A, Haschke F, Duda GN, Perka C, et al: Differential regulation of blood vessel formation between standard and delayed bone healing. J Orthop Res 27: 1133–1140, 2009
Liu X, Zhou C, Li Y, Ji Y, Xu G, Wang X, et al: SDF-1 promotes endochondral bone repair during fracture healing at the traumatic brain injury condition. PLoS One 8: e54077, 2013
Liu Y, Berendsen AD, Jia S, Lotinun S, Baron R, Ferrara N, et al: Intracellular VEGF regulates the balance between osteoblast and adipocyte differentiation. J Clin Invest 122: 3101–3113, 2012
Long X, Li X, Cheng Y, Yang X, Qin L, Qiao Y, et al: Preservation of disc for treatment of traumatic temporomandibular joint ankylosis. J Oral Maxillofac Surg 63: 897–902, 2005
Lu C, Miclau T, Hu D, Marcucio RS: Ischemia leads to delayed union during fracture healing: a mouse model. J Orthop Res 25: 51–61, 2007
Lu C, Saless N, Hu D, Wang X, Xing Z, Hou H, et al: Mechanical stability affects angiogenesis during early fracture healing. J Orthop Trauma 25: 494–499, 2011
Maes C, Kobayashi T, Selig MK, Torrekens S, Roth SI, Mackem S, et al: Osteoblast precursors, but not mature osteoblasts, move into developing and fractured bones along with invading blood vessels. Dev Cell 19: 329–344, 2010

Maes C, Carmeliet G, Schipani E: Hypoxia-driven pathways in bone development, regeneration and disease. Nat Rev Rheumatol 8: 358–366, 2012
Matsumoto T, Mifune Y, Kawamoto A, Kuroda R, Shoji T, Iwasaki H, et al: Fracture induced mobilization and incorporation of bone marrow-derived endothelial progenitor cells for bone healing. J Cell Physiol 215: 234–242, 2008
Miller GA, Page Jr HL, Griffith CR: Temporomandibular joint ankylosis: review of the literature and report of two cases of bilateral involvement. J Oral Surg 33: 792–803, 1975
Moss A: The angiopoietin:Tie 2 interaction: a potential target for future therapies in human vascular disease. Cytokine Growth Factor Rev 24: 579–592, 2013
Oe K, Miwa M, Sakai Y, Lee SY, Kuroda R, Kurosaka M: An in vitro study demonstrating that haematomas found at the site of human fractures contain progenitor cells with multilineage capacity. J Bone Jt Surg Br 89: 133–138, 2007
Oetgen ME, Merrell GA, Troiano NW, Horowitz MC, Kacena MA: Development of a femoral non-union model in the mouse. Injury 39: 1119–1126, 2008
Parikh SM: Angiopoietins and Tie2 in vascular inflammation. Curr Opin Hematol 24: 432–438, 2017
Park S, Sorenson CM, Sheibani N: PECAM-1 isoforms, eNOS and endoglin axis in regulation of angiogenesis. Clin Sci (Lond) 129: 217–234, 2015
Peters A, Schell H, Bail HJ, Hannemann M, Schumann T, Duda GN, et al: Standard bone healing stages occur during delayed bone healing, albeit with a different temporal onset and spatial distribution of callus tissues. Histol Histopathol 25: 1149–1162, 2010
Presta M, Foglio E, Churruca Schuind A, Ronca R: Long pentraxin-3 modulates the angiogenic activity of fibroblast growth factor-2. Front Immunol 9: 2327, 2018
Riddle RC, Khatri R, Schipani E, Clemens TL: Role of hypoxia-inducible factor-1alpha in angiogenic-osteogenic coupling. J Mol Med (Berl) 87: 583–590, 2009
Robins JC, Akeno N, Mukherjee A, Dalal RR, Aronow BJ, Koopman P, et al: Hypoxia induces chondrocyte-specific gene expression in mesenchymal cells in association with transcriptional activation of Sox9. Bone 37: 313–322, 2005
Sawhney CP: Bony ankylosis of the temporomandibular joint: follow-up of 70 patients treated with arthroplasty and acrylic spacer interposition. Plast Reconstr Surg 77: 29–40, 1986
Schipani E, Maes C, Carmeliet G, Semenza GL: Regulation of osteogenesis-angiogenesis coupling by HIFs and VEGF. J Bone Miner Res 24: 1347–1353, 2009
Street J, Bao M, deGuzman L, Bunting S, Peale Jr FV, Ferrara N, et al: Vascular endothelial growth factor stimulates bone repair by promoting angiogenesis and bone turnover. Proc Natl Acad Sci U S A 99: 9656–9661, 2002
Valentini V, Vetrano S, Agrillo A, Torroni A, Fabiani F, Iannetti G: Surgical treatment of TMJ ankylosis: our experience (60 cases). J Craniofac Surg 13: 59–67, 2002
Wang HL, Zhang PP, Meng L, Liang SX, Liu H, Yan YB: Preserving the fibrous layer of the mandibular condyle reduces the risk of ankylosis in a sheep model of intracapsular condylar fracture. J Oral Maxillofac Surg 76: 1951.e1–1951.e24, 2018
Wang HL, Liu H, Shen J, Zhang PP, Liang SX, Yan YB: Removal of the articular fibrous layers with discectomy leads to temporomandibular joint ankylosis. Oral Surg Oral Med Oral Pathol Oral Radiol 127: 372–380, 2019
Woodfin A, Voisin MB, Nourshargh S: PECAM-1: a multi-functional molecule in inflammation and vascular biology. Arterioscler Thromb Vasc Biol 27: 2514–2523, 2007
Xiao E, Li JM, Yan YB, An JG, Duan DH, Gan YH, et al: Decreased osteogenesis in stromal cells from radiolucent zone of human TMJ ankylosis. J Dent Res 92: 450–455, 2013
Yan YB, Duan DH, Zhang Y, Gan YH: The development of traumatic temporomandibular joint bony ankylosis: a course similar to the hypertrophic nonunion? Med Hypotheses 78: 273–276, 2012
Yan YB, Zhang Y, Gan YH, An JG, Li JM, Xiao E: Surgical induction of TMJ bony ankylosis in growing sheep and the role of injury severity of the glenoid fossa on the development of bony ankylosis. J Craniomaxillofac Surg 41: 476–486, 2013
Yan YB, Li JM, Xiao E, An JG, Gan YH, Zhang Y: A pilot trial on the molecular pathophysiology of traumatic temporomandibular joint bony ankylosis in a sheep model. Part II: the differential gene expression among fibrous ankylosis, bony ankylosis and condylar fracture. J Craniomaxillofac Surg 42: e23–e28, 2014a
Yan YB, Li JM, Xiao E, An JG, Gan YH, Zhang Y: A pilot trial on the molecular pathophysiology of traumatic temporomandibular joint bony ankylosis in a sheep model. Part I: expression of Wnt signaling. J Craniomaxillofac Surg 42: e15–e22, 2014b
Yan YB, Liang SX, Shen J, Zhang JC, Zhang Y: Current concepts in the pathogenesis of traumatic temporomandibular joint ankylosis. Head Face Med 10: 35, 2014c
Yang R, Chen Y, Chen D: Biological functions and role of CCN1/Cyr61 in embryogenesis and tumorigenesis in the female reproductive system (Review). Mol Med Rep 17: 3–10, 2018
Yu Y, Gao Y, Wang H, Huang L, Qin J, Guo R, et al: The matrix protein CCN1 (CYR61) promotes proliferation, migration and tube formation of endothelial progenitor cells. Exp Cell Res 314: 3198–3208, 2008
Zhang Y, He DM: Clinical investigation of early post-traumatic temporomandibular joint ankylosis and the role of repositioning discs in treatment. Int J Oral Maxillofac Surg 35: 1096–1101, 2006
Zhang Y, He DM, Ma XC: Posttraumatic temporomandibular joint ankylosis: clinical development and surgical management. Zhonghua Kou Qiang Yi Xue Za Zhi 41: 751–754, 2006
Zhao G, Huang BL, Rigueur D, Wang W, Bhoot C, Charles KR, et al: CYR61/CCN1 regulates sclerostin levels and bone maintenance. J Bone Miner Res 33: 1076–1089, 2018